

Cold Atom Qubits

Dmitry Solenov* and Dmitry Mozyrsky†

Theoretical Division (T-4), Los Alamos National Laboratory, Los Alamos, NM 87545, USA

(Dated: September 9, 2018)

We discuss a laser-trapped cold-atom superfluid qubit system. Each qubit is proposed as a macroscopic two-state system based on a set of Bose-Einstein condensate (BEC) currents circulating in a ring, cut with a Josephson barrier. We review the effective low energy description of a single BEC ring. In particular, it is demonstrated that such system has a set of metastable current states which, for certain range of parameters, form an effective two-state system, or a qubit. We show how this qubit can be initialized and manipulated with currently available laser-trapping techniques. We also discuss mechanisms of coupling several such ring qubits as well as measuring individual qubit-ring systems.

I. INTRODUCTION

Since the first successful experiments on Bose-Einstein condensation of alkali gases, optical cooling and trapping have become a standard experimental tool to study quantum degenerate gases at ultra-low temperatures. The laser trapping of neutral atoms has been rapidly developing over the past decade. State-of-the-art traps are capable of forming precise time-varying potentials with micron-size resolution [1]. High densities ($\sim 10^{10-13} \text{ cm}^{-3}$) and wide range of interactions have been achieved at nK temperatures [2, 3]. Not surprisingly, cold atom systems have become a perfect tool to test fundamental physics from basic quantum mechanical principles and quantum information to complex strongly correlated quantum states of matter [4–9].

Trapping of neutral atoms is based almost entirely on resonant scattering of light. It utilizes the internal energy structure of an atom to the control radiation pressure of the trapping (cooling) laser beam. An accurately configured laser field creates an effective (attractive or repulsive) potential profile for each atom, see [3, 10–13] for further details. Each atom is indistinguishable and has either integer or half-integer spin depending on its nuclear and electronic content. Hence, at the temperatures of typical cold-atom experiment, atoms obey Bose or Fermi statistics, e.g. typical “bosons” are ^{87}Rb , ^{85}Rb , ^7Li , ^{133}Cs , etc.

Quantum information has been introduced in a cold-atom system on various levels [14, 15]. It is natural, for example, to define a qubit (two state system) via two internal states of an atom. In this case, each atom records a single bit of quantum information. This approach, however, requires each atom to be addressed separately. A similar problem appears when the qubit is introduced via a set of spatially localized states (e.g. in adjacent wells of an optical lattice potential) of an atom or a dilute Bose-Einstein Condensate (BEC). The complication is due to the fact that the number of atoms, N , in a BEC (cold-atom) experiment fluctuates significantly, about 10% (or at least as \sqrt{N}), from run to run. Therefore any qubit system dependent on the number of atoms becomes problematic.

Another way to introduce a two-state system is via a collective phenomena. In this case the qubit has to be formed by a pair of distinct macroscopic states that are sufficiently far away from other states of the multiparticle system and, at the same time, have the energy difference between these lowest states small enough to allow measurable dynamics [16]. Already in the early stages, the experiments on BEC of trapped atoms were focused on the dynamics in a double-well(dot) trapping potential [17]. However, despite the appealing similarity with a single-particle two-state system, the BEC system of such geometry presents no easy way to achieve superposition of macroscopic states with measurable two-state dynamics. Consider, for example, a typical system of non-interacting (weakly interacting) boson atoms in a double-well confinement potential. At low temperatures (typically $\sim 100 \text{ nK}$) the atomic gas forms a BEC state, which is a many-particle product state $\prod_i [A\chi_L(\mathbf{r}_i) + B\chi_R(\mathbf{r}_i)]$, where $\chi_{L/R}(\mathbf{r})$ is a single particle state localized in the left/right well. This wave function is clearly not suitable to define a microscopic two state system—it describes a collection of non-interacting indistinguishable microscopic (single particle) two state systems that have been discussed earlier. A similar system with repulsive scattering favors a Mott state of type $\mathcal{P}[\prod_{i=1}^{N/2} \chi_L(\mathbf{r}_i)][\prod_{i=N/2+1}^N \chi_R(\mathbf{r}_i)]$, where \mathcal{P} denotes permutation of particle indexes. A schrodinger-cat state $A\prod_i \chi_L(\mathbf{r}_i) + B\prod_i \chi_R(\mathbf{r}_i)$ appears only in the limit of sufficiently strong attractive interaction. Such a two-state system, however, is difficult to handle. The transitions between the left and right macroscopic states are greatly suppressed. The tunneling exponent is

* E-mail: solenov@lanl.gov (the author to whom the correspondence should be addressed)

† E-mail: mozyrsky@lanl.gov

proportional to the number of particles. Coherent evolution appears on reasonable time scales only in the limit of vanishingly small barrier.

The outlined difficulties can be overcome in a two-state system defined by macroscopic states that span the same spatial region, e.g. superfluid (BEC) current states. The simplest geometry featuring such persistent current states is a ring. It is inspired by the celebrated superconducting flux qubit [16, 18, 19]—a superconductor ring with a Josephson junction. In a superconductor ring system the qubit is encoded by the magnetic flux states which are due to the supercurrent of charged particles (Cooper pairs of charge $2e$). Low energy dynamics of these states is due to an interplay of three energies: the magnetic inductive energy of the ring, the electric field charging energy, and the energy associated with the Josephson junction—a cut in the superconducting ring. Neutral atomic BEC confined in a ring featuring weak link (Josephson junction) does not have the first two of these energies. Nevertheless, it turns out that such BEC system can still mimic the behavior of superconducting Josephson ring device in certain cases [20].

In the following we address the essential physics of the BEC Josephson ring system. We derive an effective low energy description (Sec. II) and show that it is suitable to introduce a macroscopic two-state system, or qubit (Sec. III). We discuss possible approaches to single and multi-qubit dynamics (Sec. IV) and outline measurement procedures (Sec. V). We do not discuss the advantages of BEC-Josephson qubit systems over more traditional qubit designs. The goal of this investigation is to introduce an approach to quantum information based on trapped BEC persistent-current states. While we give some analysis of a BEC-based qubit and discuss basic quantum operations, we do not perform a comprehensive study of single- and multi-qubit gates. Rather, we outline basic principles and state challenges that will have to be addressed to fully understand the potentials of this system.

II. BEC-JOSEPHSON SYSTEM

In this section we present a detailed review of a single persistent-current BEC-Josephson device. The system is inspired by celebrated superconducting Josephson ring—the simplest geometry of a superconductor flux qubit [16]. The starting point for our system is a toroidal BEC [21–23]—a BEC of neutral atoms confined in a ring-shaped potential. Since the atomic system is in a Bose-condensed state it maintains phase coherence along the ring. As the result, the phase flux through the ring can change only by multiples of 2π , i.e. $2\pi\nu$. The integer ν is a winding number. It defines quantized current states: recall that the superfluid current is proportional to the gradient of phase along the ring. To have a non-integer winding number the phase has to jump discontinuously at some point along the ring (phase slip). This is possible only if the BEC density at that point vanishes. The energy cost of creating vanishing density, or a node, comes from kinetic energy and is usually high. However, if a sufficiently high potential barrier is introduced, the node can be easily created inside the barrier. As the result, the phase across the barrier can change only by a fraction of 2π , causing a small increase in energy, $\sim E_J$ (Josephson energy). The interplay of this energy with the energy of the BEC in the bulk of the ring creates rich potential landscape which can be exploited to create and manipulate persistent current states. In the following we will derive an effective low-energy action suitable to capture essential physics of persistent current states. The derivations will largely follow Ref. [20].

The system of interest is shown in Fig. 1, see also Ref [1]. As soon as atoms are cooled down to nK temperatures the trapping is achieved by two laser beams. With the appropriate detuning they can be set effectively attractive (potential is lower in region with higher light intensity). The main beam is directed horizontally, see Fig. 1(a), and focused to a few μm in the BEC region. It oscillates to the sides with frequency ~ 100 Hz. The atoms move much slower and observe only a time-averaged beam. A virtually flat 2D-plane potential well is created. The other “painting” beam scans the 2D-sheet trap from above creating time-averaged effective attractive or repulsive potential in addition to the primary 2D trap. The potential profile corresponding to the BEC-Josephson system is (schematically) shown in Fig. 1(b). It is a toroidal potential well of radius $10 - 100\mu\text{m}$ (circumference $L \sim 60 - 600\mu\text{m}$) and thickness of about $1 - 10\mu\text{m}$. The $1\mu\text{m}$ -size potential barrier is placed at some point of the toroidal well. The barrier can rotate along the ring with variable frequency (typically \sim Hz) to stir the condensate.

The trap with parameters outlined above permits several regimes of BEC dynamics: (a) Complex three-dimensional (3D) flow. If the thickness of the BEC ring is significant compared to its healing length, ξ , vortex excitations can form in the bulk of the BEC ring. This regime has been explored in [24]. (b) Quasi-one-dimensional (1D) flow along a large-circumference ring. This regime is realized when vortex excitations are squeezed to higher energies by tight (of the order of few ξ) transverse confinement, while the circumference of the ring is large so that the kinetic energy of atomic motion (BEC flow) corresponding to $\nu \sim 1$ is negligible. (c) Quasi-1D small ring limit. In this case kinetic energy of rotation plays an important role. We will focus on the quasi-1D regime of BEC dynamics, i.e. (b) and (c).

We start with the microscopic description of a quasi-1D BEC system and investigate the partition function, Z , at low temperatures,

$$Z = \text{Tr}[e^{H/k_B T}] = \int \mathcal{D}\psi^* \mathcal{D}\psi e^{-S}, \quad (1)$$

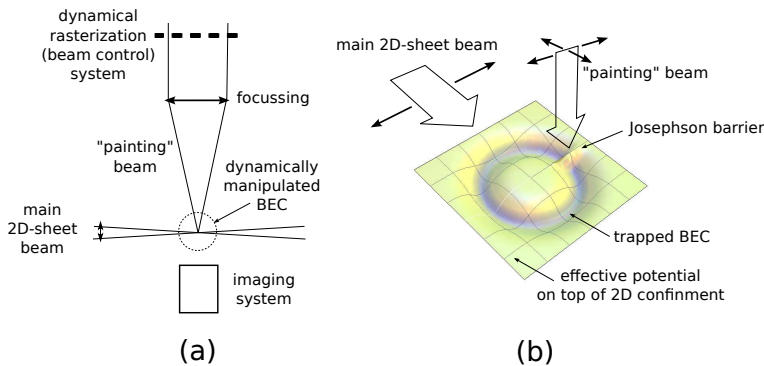


FIG. 1: (a) Essential components of dynamically manipulated "painted potential" trap [1]. (b) Ring-shaped BEC (schematically) formed in the toroidal potential well cut with the Josephson barrier. The effective (time-averaged) potential profile is created by the "painting" beam on top of 2D-sheet confinement.

where ψ is the boson field variable. Our goal is to formulate the effective action in terms of the phase difference across the junction $\phi = \varphi(0) - \varphi(L)$ integrating out other degrees of freedom. All the parameters are assumed in the units of a quasi-1D system; we also set $\hbar = 1$. The microscopic action \mathcal{S} is

$$\mathcal{S} = \mathcal{S}_0 + \mathcal{S}_{\mathcal{J}}, \quad (2)$$

$$\mathcal{S}_0 = \int_0^\beta d\tau \int_0^L dx \psi^*(x, \tau) \left[\partial_\tau - \frac{\nabla^2}{2m} + \frac{\lambda}{2} \psi^*(x, \tau) \psi(x, \tau) \right] \psi(x, \tau), \quad (3)$$

$$\mathcal{S}_{\mathcal{J}} = \int_0^\beta d\tau \mathcal{J} [\psi^*(0, \tau) \psi(L, \tau) + \psi^*(L, \tau) \psi(0, \tau)]. \quad (4)$$

Here $\beta = 1/k_B T$, and the position along the ring, x , is measured from the junction edge. It is convenient to introduce parametrization $\psi(x, \tau) = \sqrt{\rho + \delta\rho(x, \tau)} e^{i\varphi(x, \tau)}$, where ρ is the mean-field BEC density. This density is constant, $\rho = N/L$, everywhere along the ring except near the Josephson barrier where it approaches zero. Spatial variations of density in this region are lumped into the effective Josephson constant \mathcal{J} . With these definitions we obtain the standard Josephson action

$$\mathcal{S}_{\mathcal{J}} = \int_0^\beta d\tau E_J \cos \phi(\tau), \quad (5)$$

where $E_J = \mathcal{J}N/L$ is Josephson energy. Calculations for the bulk action \mathcal{S}_0 are more involved. We first rewrite \mathcal{S}_0 in terms of fluctuation fields

$$\mathcal{S}_0 = \mathcal{S}_{MF} + \int_0^\beta d\tau \int_0^L dx \left[i\delta\rho\dot{\phi} + \frac{\rho}{2m}(\nabla\phi)^2 + \frac{\lambda}{2}\delta\rho^2 + \frac{1}{8\rho m}(\nabla\delta\rho)^2 + \dots \right]. \quad (6)$$

The low-energy physics is governed by long-wave fluctuations [20, 25], i.e. ∇ -terms and also $\dot{\phi}$ are considered small. Another small parameter is the magnitude of the density fluctuations. Therefore it is appropriate to keep only the first three terms under the integral sign in Eq. (6). After this approximation the density fluctuations enter in quadratic form, $Z \sim \int \mathcal{D}\delta\rho \exp[-A\delta\rho^2]$, and can be integrated out. We obtain

$$\mathcal{S}_0 = \mathcal{S}_{MF} + \frac{1}{L} \sum_k \int \frac{d\omega}{2\pi} \frac{1}{2\lambda} [c^2 k^2 + \omega^2] \varphi^2(k, \omega), \quad (7)$$

where the velocity of sound is $c^2 = \rho\lambda_B/m$. This is the standard phonon action formulated in terms of phase fluctuations (density and phase fluctuations are conjugate variables). We will focus on the tractable limit for which sound fluctuations along the ring are bounded by the Josephson junction and, hence, quantized by the boundary condition $\partial_x \varphi(0, \tau) = \partial_x \varphi(L, \tau) = 0$. This is appropriate as soon as the level spacing $\min(ck) = 2\pi c/L$ in the excitation energy spectrum is much larger than the Josephson energy per particle E_J/N , i.e. $c \gg \mathcal{J}$. In this limit

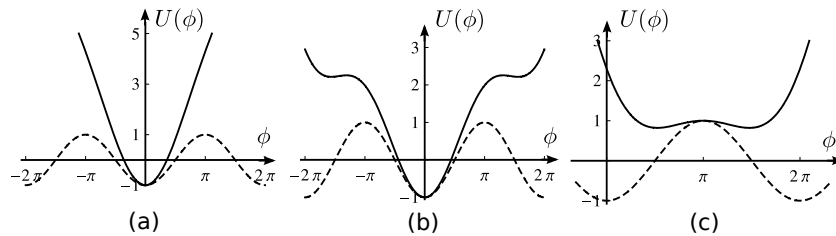


FIG. 2: Typical effective potential energy profiles (in units of E_J) as functions of the phase across the Josephson barrier. For comparison, pure Josephson energy contribution is given. (a) Josephson energy, E_J , is small compared to effective the “inductive” energy (kinetic energy of rotating BEC). (b) E_J is comparable to the effective “inductive” energy. (c) Same as (a) but with rotating Josephson barrier (in rotating frame of reference).

the action (7) can be reduced to a local action by integrating out $\varphi^2(k, \omega)$ assuming that $\phi(\omega) = \varphi(0, \omega) + \varphi(L, \omega)$. It is accomplished by introducing the functional δ -function according to

$$Z = \prod_{\omega} \int \mathcal{D}\phi \mathcal{D}\varphi e^{-\mathcal{S}[\phi(\omega) - \varphi(0, \omega) + \varphi(L, \omega)]} \quad (8)$$

and using the identity $\delta(a) = (2\pi)^{-1} \int d\Lambda \exp(i\Lambda a)$. The fields φ and z can then be integrated out. Note that in doing so we expand field $\varphi(x, \tau)$ in $\cos(\pi n x/L)$, thus satisfying the boundary conditions above. After some calculation we notice that the partition function takes the form $Z = \int \mathcal{D}\phi \exp(-\mathcal{S}_{\text{eff}})$, where

$$\mathcal{S}_{\text{eff}} = \int \frac{d\omega}{2\pi} |\phi(\omega)|^2 \frac{c\omega}{4\lambda \tanh(\frac{\omega L}{2c})} - E_J \int d\tau \cos \phi(\tau). \quad (9)$$

In the limit of large ring, $L \rightarrow \infty$ (regime (b) as discussed earlier), we recover the Caldeira-Leggett dissipative action [26, 27]

$$\mathcal{S}_{\text{eff}} \rightarrow \frac{c}{4\lambda} \int \frac{d\omega}{2\pi} |\omega| |\phi(\omega)|^2 - E_J \int d\tau \cos \phi(\tau), \quad (10)$$

which describes dissipative particle dynamics in a periodic potential.

We are interested in the “coherent” limit when L is finite and $\omega \rightarrow 0$ (regime (c) as discussed earlier). In this case we obtain

$$\mathcal{S}_{\text{eff}}^0 = \int d\tau \left[\frac{L}{24\lambda} \dot{\phi}(\tau)^2 + \frac{\rho}{2mL} \phi(\tau)^2 - E_J \cos \phi(\tau) \right]. \quad (11)$$

Note that all the terms in Eq. (11) resemble those of the superconducting flux qubit. In the latter system, however, the first two terms originate from classical electromagnetism [16]: the $\dot{\phi}$ -term, $(\hbar^2 C/8e^2)\dot{\phi}^2$, is due to the electric field of the capacitor formed by different sides of the Josephson junction (and the ring); the ϕ^2 -term, $(\hbar^2/8e^2 \mathcal{L})\phi^2$, is the result of the magnetic field energy induced by the supercurrent. In our case the kinetic term is the consequence of phonon quantization, while the ϕ^2 -term is due to the kinetic energy of the collective motion of the particles—superfluid current.

Finally, we consider the case of a rotating Josephson barrier. At this point it is already clear that the effect of rotation should contribute to the ϕ^2 -term of the above action. As we will see shortly, the rotation of the trap is indeed equivalent to a flux of external magnetic field used to tune the superconducting Josephson rings. Consider the rotation [13] of the form $V(x \cos(\Omega t) + y \sin \Omega t, x \cos(\Omega t) - y \sin \Omega t, z)$. In the rotating frame of reference $x \rightarrow x + vt$, $v = \Omega L/2\pi$. This change adds the term $\int d\tau \rho v \dot{\phi}(\tau)$ to the above action. Introducing $\alpha = m\mathcal{J}L$ we obtain

$$\mathcal{S}_{\text{eff}}^0 = E_J \int d\tau \left[\frac{L}{24\lambda E_J} \dot{\phi}(\tau)^2 + \left\{ \frac{(\phi(\tau) - \phi_0)^2}{2\alpha} - \cos \phi(\tau) \right\} \right], \quad (12)$$

where $\phi_0 = mL^2\Omega/2\pi$. The parameter α , together with ϕ_0 , determines the shape of the effective energy, i.e. the last two terms under the integral sign. Three situations are possible, see Fig. 2: (a) When the tunneling through the Josephson barrier is negligible ($\alpha \rightarrow 0$) the atomic system condenses into the rotating BEC state defined by ϕ_0 . (b) When the tunneling becomes significant the stationary system ($\Omega = 0$) develops a set of metastable current-carrying

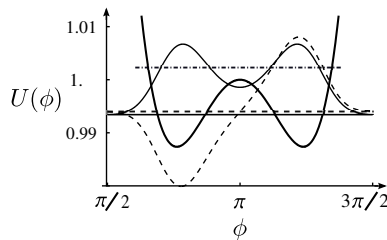


FIG. 3: Typical double-well configuration: three lowest energies and two basis qubit states are shown.

states (local minima of the effective potential). The metastable states appear when both the first and the second derivative of the effective potential with respect to ϕ vanish. The corresponding set of equations is

$$\tan \phi_{s,i} = \phi_{s,i}, \quad \alpha_i = -1/\cos \phi_{s,i}. \quad (13)$$

The first pair of metastable states appear when $\alpha > \alpha_1 \approx 4.6$ ($\phi_{s,1} \approx \pm 1.43\pi$), the second when $\alpha > \alpha_2 \approx 10.95$, and so on. (c) Finally, when rotation $\phi_0 \sim \pi$ (winding number 1/2) and $\alpha > 1$ a double-well potential forms, see Fig. 2. In this review we are interested in the latter case. The analysis of the previous two situations can be found in [20].

III. BEC CURRENT-BASED TWO-STATES SYSTEM: BEC QUBIT

A. Formulation of a two-state system

Consider the double-well regime with $\phi_0 \sim \pi$, $\alpha > 1$. Starting with the classical single-particle action (12) analytically continued to real times, we follow standard quantization procedure, see [16]. While such procedure leads to the correct result, the reader should refer to a more detailed derivation based on the analysis of the many-body wave function [28]. The Lagrangian corresponding to the real-time action is

$$\mathcal{L} = \frac{L}{24\lambda} \dot{\phi}(t)^2 - E_J U(\phi(t)), \quad (14)$$

where

$$U(\phi) = \frac{1}{2\alpha} (\phi - \phi_0)^2 - \cos(\phi). \quad (15)$$

The motion of the effective “collective” particle can be formally quantized as follows. First, we introduce canonical momentum P and perform a Legendre transformation to formulate a classical Hamiltonian description

$$P = \partial\mathcal{L}/\partial\dot{\phi} = \frac{L}{12\lambda} \dot{\phi}(t), \quad \mathcal{H} = P\dot{\phi} - \mathcal{L}. \quad (16)$$

We obtain

$$\mathcal{H} = E_J \left[\frac{1}{2\mu} P^2 + U(\phi) \right], \quad (17)$$

where $\mu = \alpha\eta^2/12$, $\eta = \sqrt{\rho/m\lambda}$. The quantization is performed introducing $P \rightarrow \hat{P} = -d/d\phi$, so that $[\hat{P}, \phi] = 1$. Finally, we arrive at the effective Schrodinger equation describing the distribution of the collective variable ϕ

$$E\psi(\phi) = E_J \hat{\mathcal{H}}\psi(\phi), \quad \hat{\mathcal{H}} = \frac{1}{2\mu} \left(-\frac{d}{d\phi} \right)^2 + U(\phi). \quad (18)$$

The above quantization procedure invokes a conceptual question [19]: The quantization is done on the quantity which is defined by purely quantum processes, such as BEC condensation, quantized phonon vibrations, and Josephson tunneling. Is it appropriate to use such quantum approach to (14) at all? A similar problem with quantization of the collective variable takes place in the standard superconducting Josephson ring [16]. In the latter case (due to complexity of the microscopic description) this question is resolved primarily by experiment. In our case it can be

done by constructing an appropriate many-body wave function. It turns out that the superposition of condensates, each corresponding to a certain value of phase ϕ , weighted by $\psi(\phi)$, reproduces Eqs. (18) exactly in the limit of large number of particles $1/N \ll 1/\eta\sqrt{\alpha-1} \ll \sqrt{N}/\eta$; further limitations on η should be enforced to maintain acceptable signal-to-noise ratio during measurement [28].

The effective potential U and the corresponding energy levels are shown in Fig. 3. When $\phi_0 \sim \pi$ the potential acquires double well shape. The splitting energy, 2ε , between the two lowest energies is controlled by the height of the barrier $\sim (\alpha-1)^{3/2}/\alpha^{3/2}$ and effective mass μ . For $\alpha-1 \ll 1$ and $\eta \sim 10-100$ the energy ε can be set an order of magnitude smaller compared to the energy gap to the third level and a two state approximation can be used. In the case of $\phi_0 = \pi$ we obtain

$$i\dot{|\psi\rangle} = H_0|\psi\rangle, \quad H_0 = \varepsilon\sigma_z, \quad (19)$$

where state $|\psi\rangle \rightarrow (0,1)^T$ corresponds to the symmetric ground state of (18) and $|\psi\rangle \rightarrow (1,0)^T$ is the first excited (antisymmetric) state. The splitting energy ε can be easily calculated numerically. An analytical estimate is $\varepsilon \sim (c/L) \exp[-2\sqrt{6}\eta(\alpha-1)^{3/2}/\alpha]$.

Finally, we should point out that the coherent description (14,18,19) relies on the effective low-energy action (11). It was obtained assuming $\omega L/c \ll 1$. At sufficiently large ω dissipative corrections become important and the "coherent" description (18) is no longer valid. In the case of the double-well configuration ($\phi_0 = \pi$) ω can be estimated as the frequency of an instanton oscillating inside the barrier (which is potential well for the instanton). We obtain $\omega \sim E_J\sqrt{\alpha-1}/\alpha\eta = c\sqrt{\alpha-1}/L$. Therefore the coherent description is appropriate for small barriers when $\alpha-1 \ll 1$. On the other hand, $\alpha-1$ should not be too small so that different ϕ states are still distinguishable during measurement.

B. Single-qubit operations and initialization

Unlike in solid-state quantum computing systems, we cannot use strong measurement procedure [29] to initialize the BEC-qubit directly. The BEC-Josephson two state system is based upon interplay of different persistent-current states. At the same time, measurement of BEC currents is usually destructive, as we will see in the last section. Hence, we should resort to an indirect measurement using a heat bath. Fortunately such measurement is inherent to the BEC cooling process—evaporative cooling: this process involves lowering the trap potential to release hot "vapor" particles; the remainder of the gas re-thermalizes due to scattering. The preparation starts with cooling of the trapped atomic gas. Depending on target winding number, two strategies exist: (i) For winding numbers $< 1/2$ the pure ring potential should be used; no additional (Josephson) barrier is initially required. (ii) For winding numbers $> 1/2$, a high impenetrable barrier should be set rotating with the frequency $\Omega > \Omega_{1/2} = \pi^2/mL^2$.

We will focus on the case (i). Upon cooling the zero-current ($\phi \sim 0$) condensate forms. Due to the effective kinetic term the condensate is in a superposition of different ϕ -states distributed in the vicinity of $\phi \sim 0$ with $\Delta\phi$ determined by the effective mass μ . As soon as the Josephson barrier is raised and set rotating by gradually increasing the frequency of rotation to satisfy $\phi_0 \approx \pi$, this distribution will be adiabatically moved to form the ground state of the double-well configuration, Fig. 3. The key is to keep control over the angular acceleration, i.e. change of Ω with time. In order to have the ground state fully occupied at all times one should keep $dU(\phi)/dt \ll (E' - E_0)$, or $\dot{\phi}_0 \ll (E_1 - E_0)$, where $E_1 - E_0$ is the gap between the first two energy levels of Eq. (18) far from the double well configuration. We obtain $mL^2\dot{\Omega}/2\pi \ll c/L$. In the vicinity of the symmetric double-well configuration ($\phi_0 = \pi$), the Landau-Zener mechanism [30] can be used to drive the system to the antisymmetric state (similar to a single particle double-well system).

To address single qubit operations consider the system close to the symmetric double well configuration with $\phi_0 \sim \pi$. In the basis of the symmetric and anti-symmetric states the Hamiltonian takes the form

$$H = \varepsilon\sigma_z + \frac{\phi_0\langle\phi\rangle_{01}}{\alpha}\sigma_x, \quad (20)$$

where $\langle\phi\rangle_{01}$ is the off-diagonal matrix element of ϕ in the same basis. Both phase and flip [29] operation can be carried out by tuning the parameters ε and ϕ_0 (i.e. the Josephson tunneling and frequency of rotation of the barrier).

IV. MULTI-QUBIT DYNAMICS

It is well known that superconducting flux qubits can be easily coupled via the magnetic field [18] generated by supercurrent in each qubit. However, all the currents in the cold-atom-based qubit are flows of neutral particle. Hence,

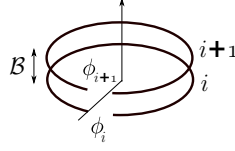


FIG. 4: Stack arrangement: BEC-Josephson rings are placed one on top of the other, so that small tunneling is present between the rings. The energy of the system is minimized when the rings are in phase.

they do not interact with electromagnetic fields. The only interaction present in the system is contact scattering. Therefore BEC-Josephson rings must come into contact with one-another or with some common (coherent) BEC media. Below we discuss the simplest stack arrangement based on this idea. While more advanced schemes are possible, we will focus on demonstrating the basic principles necessary to construct such an interaction in the simplest possible model. Multi-plane geometry, however, is not easy to implement with more than a few planes—investigation of more complex (in-plane) coupling schemes might be necessary to address the issue of scalability.

A. Interaction between a few BEC rings

Consider a stack of M similar BEC-Josephson rings placed one on top of the other in z direction (perpendicular to the 2D confinement planes) with the common axis of rotation and the same rotation frequency. The separation between the rings is such that weak tunneling is present between the equivalent parts of the adjacent rings, see Fig. 4. The Euclidian action corresponding to such configuration can be cast in the form

$$\mathcal{S}_M = \mathcal{S}_0^M + \mathcal{S}_{\mathcal{J}}^M + \mathcal{S}_{\mathcal{B}}^M. \quad (21)$$

The three components are: (i) The effective 1D action describing the bulk of each BEC ring

$$\mathcal{S}_0^M = \sum_{i=1}^M \int_0^\beta d\tau \int_0^L dx \psi_i^*(x, \tau) \left[\partial_\tau - \frac{\nabla^2}{2m} + \frac{\lambda}{2} \psi_i^*(x, \tau) \psi_i(x, \tau) \right] \psi_i(x, \tau), \quad (22)$$

(ii) The Josephson tunneling contribution for each ring in a stack

$$\mathcal{S}_{\mathcal{J}}^M = \sum_{i=1}^M \int_0^\beta d\tau \mathcal{J} [\psi_i^*(0, \tau) \psi_i(L, \tau) + \psi_i^*(L, \tau) \psi_i(0, \tau)], \quad (23)$$

(iii) The tunneling between adjacent rings in the stack

$$\mathcal{S}_{\mathcal{B}}^M = \sum_{i=1}^{M-1} \int_0^\beta d\tau \int_0^L dx \frac{\mathcal{B}}{L} [\psi_i^*(x, \tau) \psi_{i+1}(x, \tau) + \psi_{i+1}^*(x, \tau) \psi_i(x, \tau)]. \quad (24)$$

Here \mathcal{B} is the tunneling amplitude between adjacent rings. As before we assume that both $E_J = \mathcal{J}\rho$ and $E_B = \mathcal{B}\rho$ (Josephson energy due to the tunneling between the rings) are small compared to the quantized phonon excitation energies, $\min(ck) = 2\pi c/L$, in the bulk. We will also assume that all the rings in the stack are arranged such that the Josephson barriers are on top of each other. In such system the phases at the same point, x , along the rings do not change significantly between different rings $\varphi_i(x, \tau) \sim \varphi_{i+1}(x, \tau)$ —the variation of ϕ_i for each qubit state is relatively small ($\phi_i \sim \pi$) and $\varphi_i(x, \tau) \approx \phi_i x/L$ with small fluctuations around this value. We can use the hydrodynamic parametrization as before $\psi_i(x, \tau) = \sqrt{\rho + \delta\rho_i(x, \tau)} e^{i\varphi_i(x, \tau)}$ and, to the leading order in fluctuations, obtain

$$\mathcal{S}_n = \sum_i \mathcal{S}_{\text{MF}}^i + \sum_i \int dx d\tau \left[i\delta\rho_i \dot{\varphi}_i + \frac{\rho}{2m} (\nabla\varphi_i)^2 + \frac{\lambda}{2} \delta\rho_i^2 - \frac{E_B}{L} \cos(\varphi_i - \varphi_{i+1}) \right] - \sum_i \int d\tau E_J \cos \phi_i. \quad (25)$$

Here (and in the following) we suppress the arguments of the fields and the limits of the integration to shorten notation. We also expand \mathcal{S}_n to the second order in $\varphi_i(x, \tau) - \varphi_{i+1}(x, \tau)$. Higher-order corrections are irrelevant since E_B is a small quantity itself. Integrating out the density fluctuations for each ring as before, we obtain

$$\mathcal{S}_n = \sum_i \mathcal{S}_{\text{MF}}^i + \frac{1}{L} \sum_{i,k} \int \frac{d\omega}{2\pi} \left[\frac{\omega^2 + c^2 k^2}{2\lambda} |\varphi_i|^2 + \frac{E_B}{L} |\varphi_i - \varphi_{i+1}|^2 \right] - \sum_i \int d\tau E_J \cos \phi_i. \quad (26)$$

Further integration is more involved but follows the same steps as in the case of the single BEC-Josephson ring: (i) the phases ϕ_i across the junction are introduced inserting $\delta[\phi_i(\tau) - \{\varphi_i(0, \tau) - \varphi_i(L, \tau)\}]$; (ii) the δ -functions are expanded using the identity $\delta(a_i) = (2\pi)^{-1} \int d\Lambda_i \exp(i\Lambda_i a_i)$; (iii) finally, the fields φ_i and then Λ_i are integrated out (Gaussian integrals) in the same manner as before. We should note that the Gaussian integrals over φ_i are not diagonal in the index that counts different rings, hence, a diagonalization has to be done to perform the integration. Fortunately we do not have to compute these integrals since they give only a constant shift to the free energy (action) of the system which is not important here. As soon as phonon and auxiliary fields are integrated out the second sum of action (26) turns into

$$\sum_i \int \frac{d\omega}{2\pi} [K_1(\omega)|\phi_i(\omega)|^2 + E_B K_2(\omega)|\phi_i(\omega) - \phi_{i+1}(\omega)|^2], \quad (27)$$

where

$$K_1(\omega)^{-1} = \frac{1}{L} \sum_q \frac{(1 - e^{-iqL})^2}{(\omega^2 + c^2 q^2)/2\lambda} = \frac{4\lambda \tanh \frac{L\omega}{2c}}{c \omega} \quad (28)$$

and

$$K_2(\omega)^{-1} = \frac{K_1(\omega)^2}{L} \frac{1}{L} \sum_q \left[\frac{1 - e^{-iqL}}{(\omega^2 + c^2 q^2)/2\lambda} \right]^2 \xrightarrow{\omega \rightarrow 0} \frac{1}{12}. \quad (29)$$

Following Sec. II we keep only the leading frequency terms. Hence, only the zeroth order in $\omega L/c$ should be retained in $K_2(\omega)$. After some algebra we obtain the effective low-energy action describing the entire stack

$$\mathcal{S}_{\text{eff}}^M = \sum_{i=1}^M \int d\tau \left[\frac{L}{24\lambda} \dot{\phi}^2 + \frac{\rho}{2mL} \phi_i^2 + \rho v \phi_i + E_J \cos \phi_i + \frac{1}{12} E_B (\phi_i - \phi_{i+1})^2 (1 - \delta_{i,M}) \right]. \quad (30)$$

The form of this action is not surprising. Indeed, by allowing the tunneling between the rings we increase the energy of the entire system if those rings are not in phase. This is manifested (to the leading order in the phase difference) by the appearance of the last quadratic term in the action, see Eq. (30).

B. Interacting qubits

We have demonstrated that a set of M BEC-Josephson qubits can interact with the total effective energy as a function of the phase-slip phase difference given by

$$U(\phi_1, \phi_2, \dots) = \sum_{i=1}^M \left[\frac{1}{2\alpha} (\phi_i - \phi_0)^2 - \cos(\phi_i) \right] + \frac{\mathcal{B}}{\mathcal{J}} \sum_{i=1}^{M-1} (\phi_i - \phi_{i+1})^2. \quad (31)$$

However, it is still necessary to prove that potential (31) is sufficient to implement a universal set of gates [29]. Below we demonstrate that qubit-qubit coupling given by (31) together with a single qubit rotation discussed earlier can be used to implement any two-qubit gate.

Consider a stack of only two BEC-Josephson rings. In the basis of symmetric/antisymmetric states the Hamiltonian becomes

$$H = H_1 + H_2 + \frac{2\mathcal{B}\langle\phi\rangle_{01}^2}{\mathcal{J}} \sigma_x^1 \sigma_x^2, \quad (32)$$

$$H_i = \varepsilon \sigma_z^i + \left(\frac{\phi_0 - \pi}{\alpha} + \frac{2\pi\mathcal{B}}{\mathcal{J}} \right) \langle\phi\rangle_{01} \sigma_x^i. \quad (33)$$

We tune $\varepsilon \rightarrow 0$ and $\phi_0 \rightarrow \pi - 2\pi\alpha\mathcal{B}/\mathcal{J}$. In this case the evolution operator (in real time) is

$$U(t) = U_{x\sigma}^{1\dagger} U_{x\sigma}^{2\dagger} \exp \left[-i \frac{2t\mathcal{B}\langle\phi\rangle_{01}^2}{\mathcal{J}} \sigma^1 \cdot \sigma^2 \right] U_{x\sigma}^1 U_{x\sigma}^2. \quad (34)$$

Apart from single qubit rotation $U_{x\sigma}$: $\sigma_x \rightarrow \sigma = \{\sigma_x, \sigma_y, \sigma_z\}$ this is a natural representation [31] of a (SWAP) $^\xi$ gate with $\xi = 2t\mathcal{B}\langle\phi\rangle_{01}^2/\mathcal{J}$. This gate, in combination with single-qubit rotations, is sufficient to implement any two-qubit gate [31]. For instance, one CNOT gate can be realized with the help of two (SWAP) $^{1/2}$ and single-qubit gates [32].

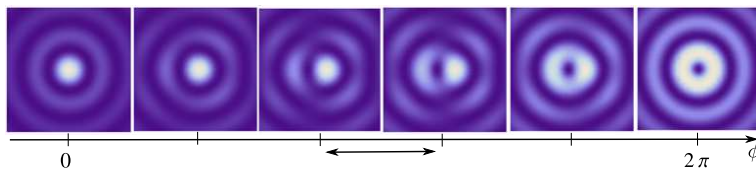


FIG. 5: Calculated Time-of-Flight (TOF) measurement outcomes. During the TOF measurement BEC-Josephson qubit wave function should collapse to a certain ϕ state. The density distribution of that state can be captured by absorption imaging during the TOF expansion. The two-way arrow indicates typical range of ϕ expected for measurable two-state BEC-Josephson system.

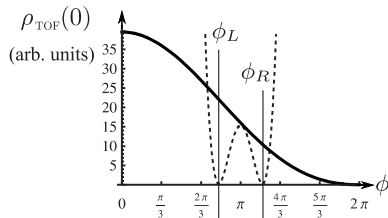


FIG. 6: Time-of-Flight density (calculated) at the center as a function of the phase-slip ϕ of the ring system before the expansion. A typical effective potential corresponding to BEC-Josephson qubit configuration is shown for comparison ($\phi_{L/R}$ marks the average position of states in the effective two state system).

V. MEASUREMENT

The only reliable mechanism to measure a cold atom system is via observation of its density. Moreover the atomic cloud has to undergo significant expansion before images with sufficient spacial resolution can be obtained. The latter is usually accomplished by Time-of-Flight (TOF) experiments [13]: the trapping potential is turned off and the density of the atomic cloud is measured after some time of free expansion. As soon as the confinement potential is off, the system is just a collection of atoms that will fly away from the position of the trap, each with the momentum supplied by the confinement and motion within the trap. Due to the tight confinement, the released atoms acquire substantial velocities which triggers fast expansion and decrease of density. The scattering between particles can be neglected, since it usually leads to effects on a much longer time scale. The wave function of the free-expanding BEC is

$$\Psi(\mathbf{r}_1, \mathbf{r}_2, \dots, t) = \int \frac{d\mathbf{p}_1}{(2\pi)^3} \frac{d\mathbf{p}_2}{(2\pi)^3} \dots \Psi(\mathbf{p}_1, \mathbf{p}_2, \dots) e^{i\mathbf{r}\mathbf{p} - i(p^2/2m)t}, \quad (35)$$

At sufficiently large times only terms with $\mathbf{r} \sim \mathbf{p}t/2m$ contribute to the integral. As the result, TOF measurement provides an image of the density in momentum space. This is ideal to capture the distribution over different current states present in (18). Consider different moments of density in the momentum space $m_n = \langle \hat{\rho}(\mathbf{q}_1) \dots \hat{\rho}(\mathbf{q}_n) \rangle$, where $\hat{\rho}(\mathbf{q}) = \int d\mathbf{r} d\mathbf{r}' e^{i\mathbf{q}(\mathbf{r}-\mathbf{r}')} \hat{\psi}^\dagger(\mathbf{r}') \hat{\psi}(\mathbf{r})$,

$$m_n = \int \mathcal{D}\psi^* \mathcal{D}\psi \int d\mathbf{r}_1 d\mathbf{r}'_1 \dots d\mathbf{r}_n d\mathbf{r}'_n e^{i\mathbf{q}_1(\mathbf{r}_1 - \mathbf{r}'_1)} \dots e^{i\mathbf{q}_n(\mathbf{r}_n - \mathbf{r}'_n)} \psi^*(\mathbf{r}'_1, 0) \psi(\mathbf{r}_1, 0) \dots \psi^*(\mathbf{r}'_n, 0) \psi(\mathbf{r}_n, 0) e^{-\mathcal{S}}. \quad (36)$$

Here \mathcal{S} is given by Eqs. (3) and (4). The expansion in terms of small fluctuations $\psi(\mathbf{r}, \tau) = \chi_{\phi(\tau)}(\mathbf{r}) + \delta\psi(\mathbf{r}, \tau)$ yields

$$m_n = \int d\phi P(\phi) |\chi_{\phi}(\mathbf{q}_1)|^2 \dots |\chi_{\phi}(\mathbf{q}_n)|^2 + g^2 [f(\mathbf{q}_1, \mathbf{q}_2) + f(\mathbf{q}_2, \mathbf{q}_3) + \dots] + \mathcal{O}(g^4), \quad (37)$$

where the (path) integrals over ϕ with $\tau \neq 0$ has been lumped into $P(\phi)$. The function $f(\mathbf{q}, \mathbf{q}')$ is a combination of two particle Green's functions describing scattering processes in and out of the condensate, see [33]. These two-particle correlations are suppressed [13] by the gas parameter $\sim g$, which limits the resolution of the measurement. For the range of parameters appropriate for the macroscopic two state BEC-Josephson system the gas parameter is small. Apart from the g^2 correction, moments (38) define a stochastic process: $P(\phi)$ plays the role of the probability to find the system at state ϕ as the result of the measurements. Hence, by measuring the density distribution in momentum space (via TOF) we measure the value of ϕ . At each experimental run a different density distribution is expected with the probability determined by $|\psi(\phi)|^2$.

The possible TOF measurement outcomes are given in Fig 5, where we plot the momentum-space density distributions $|\chi_\phi(\mathbf{q})|^2$ for several values of ϕ from 0 to 2π . Different ϕ states are clearly distinguishable. For a more quantitative judgment we propose to measure the TOF density at the center of the trap. The central TOF density, $|\chi_\phi(0)|^2 = |\int d\mathbf{r}\chi_\phi(\mathbf{r})|^2$, depends on the phase $\varphi(\mathbf{r})$ in a straightforward way. In the bulk of the ring this phase is linear (in this case kinetic energy is minimized) $\varphi(\mathbf{r}) = \phi x/L$ and, hence, $\chi_\phi(\mathbf{r}) \sim e^{i\phi x/L}$. As the result we obtain

$$\rho_{TOF}(0) = \rho_{TOF}^{\phi=0}(0) \frac{\sin^2(\phi/2)}{(\phi/2)^2}. \quad (38)$$

For the variation of ϕ relevant to the BEC-Josephson qubit system, see Fig 6, this is an approximately linear function $4/\pi^2 - 8(\phi - \pi)/\pi^2$.

In this review we have considered only the very basic properties of the cold atom BEC-Josephson rings relevant to quantum information. A detailed investigation is necessary to assess noise effects as well as scalability. A simple proof-of-principle experiment with a single BEC-Josephson macroscopic two-state system should also be helpful in determining the direction for further theoretical development.

Acknowledgments

We thank M. G. Boshier, I. Martin, V. Privman and E. Timmermans for valuable discussions and comments. DS acknowledges stimulating conversations with R. Kalas. The work is supported by the US DOE.

-
- [1] K. Henderson, C. Ryu, C. MacCormick and M. G. Boshier, *New J. Phys.* **11**, 043030 (2009).
 - [2] E. A. Donley, N. R. Claussen, S. L. Cornish, J. L. Roberts, E. A. Cornell, C. E. Wieman, *Nature* **412**, 295 (2001).
 - [3] A. E. Leanhardt, T. A. Pasquini, M. Saba, A. Schirotzek, Y. Shin, D. Kielpinski, D. E. Pritchard, W. Ketterle, *Science* **301**, 1513 (2003).
 - [4] P. P. Orth, I. Stanic, and K. Le Hur, *Phys. Rev. A* **77**, 051601 (2008).
 - [5] R. M. Kalas, A. V. Balatsky, D. Mozyrsky, *Phys. Rev. B* **78**, 184513 (2008).
 - [6] D. H. Santamore, E. Timmermans, *Phys. Rev. A* **78**, 013619 (2008).
 - [7] D. Solenov and D. Mozyrsky, *Phys. Rev. Lett.* **100**, 150402 (2008).
 - [8] D. Solenov and D. Mozyrsky, *Phys. Rev. A* **78**, 053611 (2008).
 - [9] R. M. Kalas, D. Solenov, E. Timmermans, *Phys. Rev. A* **81**, 053620 (2010).
 - [10] S. Chu, *Rev. Mod. Phys.* **70**, 685 (1998).
 - [11] C. N. Cohen-Tannoudji, *Rev. Mod. Phys.* **70**, 707 (1998).
 - [12] W. D. Phillips, *Rev. Mod. Phys.* **70**, 721 (1998).
 - [13] A. J. Leggett, *Rev. Mod. Phys.* **73**, 307 (2001).
 - [14] J. V. Porto, S. Rolston, B. Laburthe Tolra, C. J. Williams and W. D. Phillips, *Phil. Trans. R. Soc. Lond. A* **361**, 1417 (2003).
 - [15] N. Lundblad, J. M. Obrecht, I. B. Spielman, J. V. Porto, *Nature Physics* **5**, 575 (2009).
 - [16] A. J. Leggett, *Quantum mechanics at the macroscopic level*, Ecole d'été de physique théorique (Les Houches, Haute-Savoie, France) (46th: 1986)
 - [17] M. R. Andrews, H-J. Miesner, D. M. Stamper-Kurn, J. Stenger, and W. Ketterle, *Phys. Rev. Lett.* **82**, 2422 (1999).
 - [18] M. Tinkham, *Introduction to Superconductivity* (Dover Publications, New York; 2nd Edition, 2004) and references therein.
 - [19] V. Ambegaokar, U. Eckern and G. Schon, *Phys. Rev. Lett.* **48**, 1745 (1982).
 - [20] D. Solenov, D. Mozyrsky, *Phys. Rev. Lett.* **104**, 150405 (2010).
 - [21] B. P. Anderson, K. Dholakia, and E. M. Wright, *Phys. Rev. A* **67**, 033601 (2003).
 - [22] S. Gupta, K.W. Murch, K. L. Moore, T. P. Purdy, and D. M. Stamper-Kurn, *Phys. Rev. Lett.* **95**, 143201 (2005).
 - [23] C. Ryu, M. F. Andersen, P. Clade, Vasant Natarajan, K. Helmerson, and W. D. Phillips, *Phys. Rev. Lett.* **99**, 260401 (2007).
 - [24] F. Piazza, L. A. Collins, and A. Smerzi, *Phys. Rev. A* **80**, 021601 (2009).
 - [25] H.P. Buchler, V.B. Geshkenbein, and G. Blatter, *Phys. Rev. Lett.* **87**, 100403 (2001).
 - [26] A. J. Leggett, S. Chakravarty, A. T. Dorsey, M. P. A. Fisher, A. Garg, and W. Zwerger, *Rev. Mod. Phys.* **59**, 1 (1987).
 - [27] U. Weiss, *Quantum Dissipative Systems* (World Scientific, Singapore, 1999).
 - [28] D. Solenov, D. Mozyrsky, *Phys. Rev. A* **82**, 061601(R) (2010).
 - [29] M. Nielsen and I. Chuang, *Quantum Computation and Quantum Information* (Cambridge University Press, Cambridge, 2000).
 - [30] C. Zener, *Proc. of the Royal Society of London A* **137-833**, 696 (1932).
 - [31] H. Fan, V. Roychowdhury, and T. Szkopek, *Phys. Rev. A* **72**, 052323 (2005).
 - [32] D. Loss and D. P. DiVincenzo, *Phys. Rev. A* **57**, 120 (1998).

- [33] A. A. Abrikosov, L. P. Gorkov, and I. E. Dzyaloshinski, *Methods of quantum field theory in statistical physics* (Dover Publications, New York, 1975).